Structural Chemistry (2021) 32:2271–2281
https://doi.org/10.1007/s11224-021-01802-1

ORIGINAL RESEARCH

The antioxidative potential of benzofuran-stilbene hybrid derivatives: a comparison between natural and synthetic compounds

Phan Thi Thuy[1] · Nguyen Van Trang[2] · Dau Xuan Duc[1] · Ninh The Son[3]

Received: 24 May 2021 / Accepted: 13 June 2021 / Published online: 19 June 2021

Abstract

The antioxidative activity of natural product compound amurensin H (**1**) and its three synthetic compounds 5-(6-hydroxy-2-(4-hydroxyphenyl)benzofuran-3-yl)benzene-1,3-diol (**2**), (*E*)-2-(4-hydroxyphenyl)-4-(4-hydroxystyryl)benzofuran-6-ol (**3**), and (*E*)-5-(6-hydroxy-4-(4-hydroxystyryl)benzofuran-3-yl)benzene-1,3-diol (**4**) are extensively studied by DFT (density functional theory) method. At the theoretical B3LYP/6-311G(d,p) level, the HAT (hydrogen atom transfer) mechanism is assignable to compounds **1-4** in gas, but the SPL-ET (sequential proton loss-electron transfer) mechanism is the main way in water and methanol. The antioxidative actions of the studied compounds are mainly based on OH bond breakage, especially OH groups directly substituted at benzofuran nucleus. Amurensin H (**1**) is better than the remaining compounds due to 6-OH group. **1**-6-OH induces the low bond BDE (bond dissociation enthalpy) and PA (proton affinity) values in thermal analysis. Importantly, the kinetic reaction of **1**-6-OH + $HOO^{\bullet}$ in methanol exerts the lowest $\Delta G^{\#}$ value of 5.6 kcal/mol and the highest *K* value of 1.983 x 10^{10} L/mol.s. At the B3LYP/6-311G(d,p)/LANL2DZ level, the successful formation of complex [Zn(compound **1**)$_2$(H_2O)$_2$] at 6-OH is confirmed by molecular orbital and UV-Vis spectroscopic analyses.

Keywords Benzofuran · Stilbene · Hybrid · Antioxidant · Density functional theory

Introduction

In recent years, there has been a lot of interest in free radicals and related species. They were primarily arisen from ROS (reactive oxygen species) and were produced in our bodies by a variety of endogenous systems, as well as exposure to various physicochemical agents [1]. Free radicals may harm lipids, proteins, and DNA in direction [2]. As a result, the search for new drugs to combat these oxygen radicals has piqued scientist's attention.

Amurensins A–M are chemical oligostilbenes found in *Vitis amurensis* species [3, 4]. They are recognized to be the hot agents for drug developments due to their pharmacological values, especially in terms of antioxidative actions. For instance, amurensins G and B were set to have the IC_{50} values of 39.6–52.8 μM against lipid peroxidation, as compared with that of the positive control α-tocopherol (IC_{50} 9.8 μM) [5]. Amurensin H (**1**) can be thought of as a benzofuran-stilbene hybrid. Compound **1** was a promising agent against pathogenic micro-bacterial strains and anti-inflammatory diseases [6, 7]. 5-(6-Hydroxy-2-(4-hydroxyphenyl)benzofuran-3-yl)benzene-1,3-diol (**2**), (*E*)-2-(4-hydroxyphenyl)-4-(4-hydroxystyryl)benzofuran-6-ol (**3**), and (*E*)-5-(6-hydroxy-4-(4-hydroxystyryl)benzofuran-3-yl)benzene-1,3-diol (**4**) have been successfully synthesized and can be identified as derivatives of compound **1** with functional moieties deleted at carbons C-5, C-2, and C-3, respectively (Fig. 1) [6]. Compounds **2-4** have also demonstrated antimicrobial activity [6].

However, no experimental or computational studies using these compounds in antioxidative estimations have been published, to the best of our knowledge. In the current paper, the density functional theory (DFT) approach has been performed at the theoretical B3LYP/6-311G(d,p) level to discover and calculate figurative chemical parameters able to explain the electronic, structural features that might be related to free

✉ Ninh The Son
yamantson@gmail.com

[1] School of Natural Sciences Education, Vinh University, Vinh, Vietnam

[2] Institute for Tropical Technology, VAST, 18 Hoang Quoc Viet, Caugiay, Hanoi, Vietnam

[3] Institute of Chemistry, Vietnam Academy of Science and Technology (VAST), 18 Hoang Quoc Viet, Caugiay, Hanoi, Vietnam

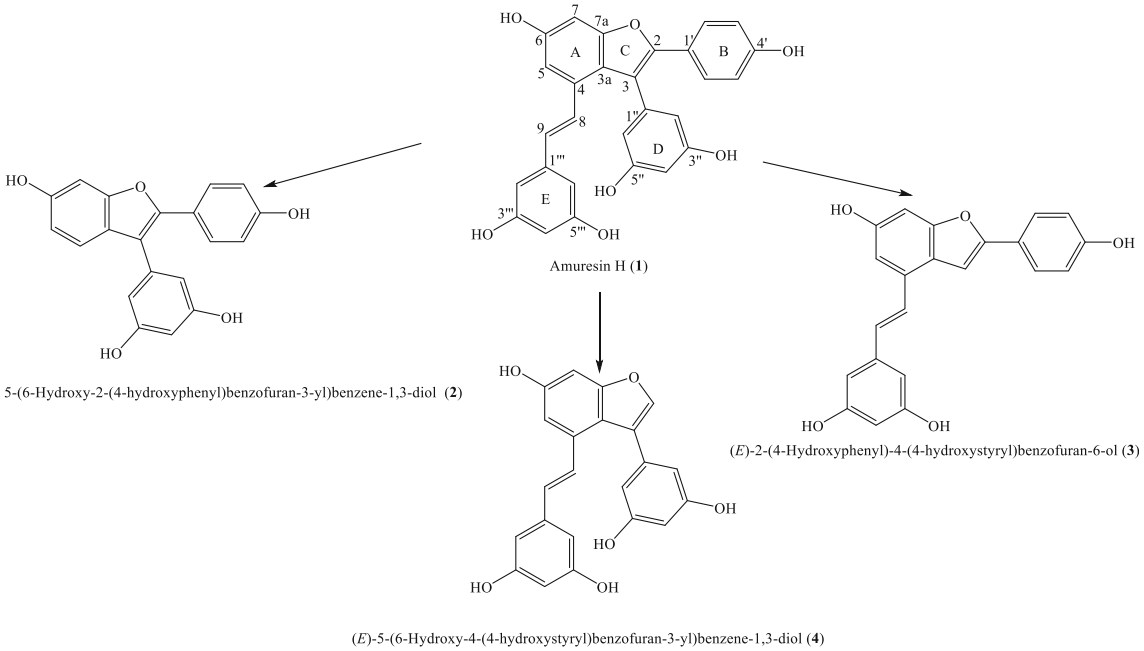

Fig. 1 General structures of compounds **1-4** with atom numbering

radical quenching of compounds **1-4**. The results also illustrate, mostly based on thermodynamically calculated considerations, a comparison between natural product **1** and synthetic compounds **2-4** in the antioxidative treatments.

Theoretical methodology

All of the DFT chemical calculations were carried out using Gaussian 09 software suite [8–17], at the theoretical B3LYP/6-311G(d,p) level [17]. Geometric optimization of a general compound X-OH and its radicals, radical cations, and anions was administered in water (dielectric constant ε = 78.34), methanol (ε = 32.60), benzene (ε = 2.27), and gas (ε = 1). Vibrational frequency analysis was also considered at the same B3LYP/6-311G(d,p) level, which ensured that the ground state was in conjunction with absence of imaginary frequency. The SCRF-PCM (self-consistent reaction field polarizable continuum method) served as a useful model to view the effect of solvents.

As reported in the various publications [1, 2, 10–17], three common mechanisms have been proposed to justify the radical scavenging capacity of compound X-OH.

The HAT mechanism (the hydrogen atom transfer) This pathway can occur since a proton from X-OH is disrupted and promptly transferred to free radical $X_1^{\bullet}$ (Eq. 1). This process is classified as a homolytic reaction and can be evaluated by the BDE-bond dissociation enthalpy (Eq. 2).

$$X{-}OH + X_1^{\bullet} \rightarrow X{-}O^{\bullet} + X_1H \quad (1)$$

$$BDE = \Delta H(X{-}O^{\bullet}) + \Delta H(H^{\bullet}) - \Delta H(X{-}OH) \quad (2)$$

The SET-PT mechanism (the single electron transfer-proton transfer) There are two stages in the SET-PT pathway (Eq. 3). The first stage is characterized by the IP-ionization potential, which is caused by the loss of an electron from X-OH to give $X\text{-}OH^{\bullet+}$ (Eq. 4). In the second stage, $X\text{-}OH^{\bullet+}$ is then deprotonated, resulting in the heterolytic process, which is defined by the PDE-proton dissociation enthalpy (Eq. 5).

$$X{-}OH + X_1^{\bullet} \rightarrow X{-}OH^{\bullet+} + X_1^{-} \rightarrow X{-}O^{\bullet} + X_1H \quad (3)$$

$$IP = \Delta H(X{-}OH^{+\bullet}) + \Delta H(e^{-}) - \Delta H(X{-}OH) \quad (4)$$

$$PDE = \Delta H(X{-}O^{\bullet}) + \Delta H(H^{+}) - \Delta H(X{-}OH^{\bullet+}) \quad (5)$$

The SPL-ET mechanism (the sequential proton loss-electron transfer) The SPL-ET route has also two stages, as shown in Eq. 6. Since A-OH was deprotonated to produce the anion $X\text{-}O^{-}$, the first stage has occurred. Since the anion $X\text{-}O^{-}$ transferred an electron to free radical $X_1^{\bullet}$, the second stage has begun. For the first and second steps, the PA (proton affinity) and ETE (electron transfer enthalpy) are used to quantify energies (Eqs. 7–8).

$$X{-}OH \rightarrow X{-}O^{-} + H^{+}; X{-}O^{-} + X_1^{\bullet} \rightarrow X{-}O^{\bullet} + X_1^{-}; X_1^{-} + H^{+} \rightarrow X_1H \quad (6)$$

$$PA = \Delta H(X{-}O^{-}) + \Delta H(H^{+}) - \Delta H(X{-}OH) \quad (7)$$

$$ETE = \Delta H(X{-}O^{\bullet}) + \Delta H(e^{-}) - \Delta H(X{-}O^{-}) \quad (8)$$

Regarding the DFT approach, $\Delta H(\mathrm{Y})$ denotes the total enthalpy of species Y, and it can be written as Eq. 9 [10, 11].

$$\Delta H(\mathrm{Y}) = \mathrm{E} + \mathrm{ZPE} + \Delta H_{\mathrm{trans}} + \Delta H_{\mathrm{rot}} + \Delta H_{\mathrm{vib}} + \mathrm{RT} \quad (9)$$

where E and ZPE stand for electronic and zero-point energies, respectively. The translational, rotational, and vibrational contributions to enthalpy are $\Delta H_{\mathrm{trans}}$, ΔH_{rot}, and ΔH_{vib}, respectively. The $\Delta H(e^-)$ and $\Delta H(H^+)$ are derived from published sources [10–17].

The antioxidative activity of molecule X-OH might be also predicted using global chemical indices [10–17] such as $\varepsilon_{\mathrm{HOMO}}$ (the highest occupied molecular orbital energy), $\varepsilon_{\mathrm{LUMO}}$ (the lowest unoccupied molecular orbital energy), spin density, MEP (molecular electrostatic potential), chemical hardness η, chemical potential μ, electronegativity χ, the electrophilicity ω, and the Fukui functions.

Based on the Koopmans theorem and finite difference approximation, these physicochemical indices can be expressed as Eqs. 10–14.

$$\eta \approx (\varepsilon_{\mathrm{LUMO}} - \varepsilon_{\mathrm{HOMO}})/2 \quad (10)$$

$$\mu \approx (\varepsilon_{\mathrm{HOMO}} + \varepsilon_{\mathrm{LUMO}})/2 = -\chi \quad (11)$$

$$\omega = \mu^2/2\eta \quad (12)$$

$$\omega^- = -(3\varepsilon_{\mathrm{HOMO}} + \varepsilon_{\mathrm{LUMO}})^2/[16(\varepsilon_{\mathrm{HOMO}} - \varepsilon_{\mathrm{LUMO}})] \quad (13)$$

$$\omega^+ = -(\varepsilon_{\mathrm{HOMO}} + 3\varepsilon_{\mathrm{LUMO}})^2/[16(\varepsilon_{\mathrm{HOMO}} - \varepsilon_{\mathrm{LUMO}})] \quad (14)$$

The Fukui functions denote the electron density after accepting or denoting an electron, by which it may estimate where the most nucleophilic (f_a^-), electrophilic (f_a^+), or radical (f_a^o) sites on a substance are (Eqs. 15–17).

The Fukui index for nucleophilic attack, f_a^+, is given for when an electron was added

$$f_a^+ = \mathrm{P_a(S+1)} - \mathrm{P_a(S)} \quad (15)$$

The Fukui index for electrophilic attack, f_a^-, is given for when an electron was removed

$$f_a^- = \mathrm{P_a(S)} - \mathrm{P_a(S-1)} \quad (16)$$

Lastly, f_a^o is denoted for radical attack

$$f_a^o = [\mathrm{P_a(S+1)} - \mathrm{P_a(S-1)}]/2 \quad (17)$$

where P represents the gross charge of atom in a substance. The electronic populations of an atom in neutral, anionic, and cationic forms are $\mathrm{P_a(S)}$, $\mathrm{P_a(S+1)}$, and $\mathrm{P_a(S-1)}$, respectively.

In the conventional transition state theory (TST) at T = 298.0 K, the functional B3LYP is also an excellent choice for kinetic estimation [10–17]. The rate constant K in a radical reaction is related to the $\Delta G^{\#}$ (the Gibbs activation energy), the Wigner coefficient κ, the Planck constant h, and the Boltzmann constant k_B through Eq. 18.

$$k(\mathrm{T}) = \kappa \frac{\mathrm{T}.k_B}{h} e^{\frac{-\Delta G^{\#}}{RT}} \quad (18)$$

Results and discussion

Geometrical analysis

A thorough understanding of the geometrical properties of the studied compounds **1-4** is critical for describing their free radical scavenging behavior. It also noted that OH groups in aromatic compounds are more and more being involved in homolytic reactions rather than aromatic methine groups; thereby, evaluating the role of OH groups is necessary [13]. The structural geometry of each compound did not differ at the DFT/B3LYP/6-311G(d,p) level in all four studied media (Fig. S1). It is possible to observe that the π-electrons are distributed in the rings of all four compounds **1-4**, as well as in the double bonds of compounds **1**, **3**, and **4**. The derivative **3** with dihedral angle θ_{11}(C3-C2-C1′-C2′) ≈ 0° is mostly planar, but the remaining compounds have lost their planar property (Table S1). Compound **1** contains θ_{11} = −20.4 to −18.2° and θ_{12}(C2-C3-C1″-C2″) ≈ −72.0°, while compound **2** accompanies by θ_{11} = −25.0 to −20.8° and θ_{12} = −58.9 to −53.5°, and compound **4** associates with θ_{12} = −62.5 to −55.9°. According to Cai et al. (2014), planar substances always have higher antioxidative activity [18]. So, compound **3** is preferable for a better outcome. The lengths of the O-H bonds in each compound range from 0.962 to 0.972 Å. When converted from gas to liquid, the O-H bond lengths in compounds **1-4** increase by 0.001–0.002 Å. The solvent, as expected, decreased the bond disruption energy.

Frontier molecular orbital (FMO) theory, molecular electrostatic potential (MEP), and spin density

It denotes that the FMO analysis is one of the quickest methods for viewing the electron contribution and predicting the best sites for antioxidative reactions since H-breakage directly concerned electron transfer [10]. Figure S2 illustrates the FMO images for both neutral and radical forms. The FMO in each compound has no difference between gas and liquids. The electrons in **2** and **4**-HOMO neutrals are set to have a similarity to their LUMO neutrals, whereas the electron concentrations in ring B of **1** and **3**-LUMO neutrals are less than those in their HOMO neutrals. In each compound, it can be generally viewed that the electrons are always highly concentrated in benzofuran nucleus (system ring AC) in both the FMO neutral and radical cases. It resembles neutrals, and the

electrons are absent (or little) in ring D of HOMO and LUMO of **1**-radicals and **4**-radicals and HOMO of **2**-radicals. In contrast to neutral, the electrons have rarely distributed in ring B of 3-4′-OH radical and ring E of **3**-3‴-OH and **3**-5‴-OH radicals. It may be possible to conclude that benzofuran nucleus (ring AC) promotes radical formation rather than phenyl units. In another way, the increase of ε_{HOMO} and the decrease of ε_{LUMO} will cause the better $\varepsilon_{gap} = \varepsilon_{HOMO} - \varepsilon_{LUMO}$. As shown in Table S2, the transfer of gas into liquids has given rise to the increase of either ε_{HOMO} or ε_{LUMO} in each compound. By this mean, the ε_{gap} in polar solvents methanol and water was found lower than that in weak polar benzene or nonpolar gas (Fig. S3). Hence, polar liquids may be the main factor affecting ionization potentials [2].

MEP pictorial surface denotes a molecule's charges in a 3D model. MEP is characterized by hue, by which red and yellow describe the abundant electrons (electrophilic), blue has shown the positive charge at max, and green stands for noncharge [10]. From Fig. S4, carbon and hydrogen atoms associate with green or blue, but oxygen atoms have induced yellow. As a consequence, OH groups set nucleophilic character.

Spin density is an important parameter to consider the speed of free radical scavenging. Rings with more spin density distribution will support radical formation better. In general, the gaseous spin density is found to delocalize at phenyl units containing O•-radical (Fig. S5). For instance, 6-OH radicals of compounds **1-4** consist of the high distribution of spin density in benzofuran nucleus. Especially, the gaseous spin density varies correspondingly to the BDE, in which O•-atom having a lower spin density yields the lower BDE [10–17]. As can be seen, 6-O• in compounds **1-4** and 4′-O• in compounds **1-3** accompany by lower spin density than other cases. Therefore, the energies for 6-OH and 4′-OH breakages are expected to be lower.

Electronic property

The η value is a useful chemical index in predicting the prevention of charge transmission [13]. It is similar to stilbenoids and alkaloids [2, 13]; four compounds **1-4** induce η in nonpolar gas and weak polar benzene higher than those in polar solvents methanol and water (Table S2). In each environment, the η values are ordered as compound **3** < **1** < **4** < **2**. It is opposite with the η values; the calculated polarizabilities of each compound in methanol and water are much higher than those in benzene and gas. According to HSAB (hard and soft acids and bases) regulation, the environment will respond to a transition from high oxidative state/low polarizability to low oxidative state/high polarizability [2, 12, 16].

The χ parameter describes the proclivity of an atom to attack the electrons and is opposite with the μ value (Eq. 11). The χ number of each studied compound has the same trend with polarizability, by which the χ values in methanol and water are always higher than in benzene and gas. It suggests that polar liquids are advantageous conditions to ionization and electron transfer. The ω descriptor has indicated the capacity of a substance's electron acceptance from its surrounding [2, 16]. The high ω^+ and ω^- values represent the electrophilic and nucleophilic properties, respectively. From Table S2, all the ω, ω^+, and ω^- values of each studied compound have scaled up with the increase of polar environment. Furthermore, the ω^- values are always superior to the ω^+ values in each medium, thereby revealing compounds **1-4** prefer to give electrons rather than accept.

One of the quick ways to consider a reactive site is the Fukui functionals. $\Delta f_a = f_a^+ - f_a^- > 0$ is indicative for electrophilicity, but $\Delta f_a < 0$ characterizes for nucleophilicity [12]. The computational Fukui descriptors of compounds **1-4** were shown in Table S3. Carbon atoms exhibit two sides. As a representative example, carbon C-2 in all four compounds **1-4** is in association with $\Delta f_a < 0$, but C-7 and C-4′ are accompanied by $\Delta f_a > 0$. Hydroxyl groups of benzofuran nucleus and ring B are characterized by $\Delta f_a < 0$, but these of other rings set two sides. $f_a^o < 0$ is used to determine the competence of radical production [12]. Only 6-OH group has generated $f_a^o < 0$, while the other OH groups failed to do so. It is desirable that 6-OH joints to radical reactions better than analogs.

Antioxidant mechanisms

The HAT route

The computational O-H BDE values for four studied compounds **1-4** in the gaseous and liquid phases are provided in Table 1. It corresponds to the findings of geometry and spin density; 6-OH and 4′-OH have the gaseous BDE values lower than those of the other OH groups in each compound. Especially, the lowest BDE values are assigned to 6-OH group of compounds **1-3**; they range from 74.5 to 77.8 kcal/mol in the studied mediums. The highest BDE values can be found in OH group of rings D and E; e.g., **1**-3‴-OH and **4**-3‴-OH have shown to contain the highest BDE values of 83.5–86.9 kcal/mol. It noted that the BDE value of each OH group in benzene mostly equalize that in water and about 2.0 kcal/mol lower than those in gas and methanol. At the same theoretical B3LYP/6-311G(d,p) level, Sadasivam and Kumaresan identified that the BDE values of OH groups of well-known antioxidative flavonoids chrysoeriol and hispidulin were to be 91.0–109.9 kcal/mol in benzene and water, which are higher than those compounds **1-4** [19]. Therefore, derivatives **1-4** might be thought as of promising antioxidative agents.

The SET-PT and SPL-ET routes

The SET-PT route consists of two steps, but it is mostly decided by the first step [9–17]. This inference is also applied to

Table 1 The phases reaction enthalpies at 298K for radicals of compounds 1-4 at the B3LYP/6-311G(d,p) level (in kcal/mol)

Compounds	BDE				IP				PDE			
	Gas	Benzene	Methanol	Water	Gas	Benzene	Methanol	Water	Gas	Benzene	Methanol	Water
1-6-OH	77.8	75.4	77.6	75.5	147.5	129.8	99.2	94.2	246.1	47.7	24.4	28.7
1-4′-OH	78.1	75.9	78.2	75.9					246.4	48.1	24.9	29.2
1-3″-OH	85.2	83.5	85.6	83.4					253.5	55.7	32.4	36.7
1-5″-OH	82.8	79.1	84.4	82.2					251.2	61.3	31.1	35.5
1-3‴-OH	86.5	84.3	86.0	83.8					254.8	56.5	32.8	37.0
1-5‴-OH	82.6	80.8	83.5	81.4					250.9	53.0	30.3	34.6
2-6-OH	76.7	74.5	76.6	74.6	151.9	132.4	100.6	95.5	240.6	44.2	22.2	26.5
2-4′-OH	78.0	76.0	78.1	75.9					241.9	45.5	23.5	27.9
2-3″-OH	84.3	82.6	84.7	82.5					248.2	52.1	30.1	34.4
2-5″-OH	83.5	81.8	84.3	82.2					247.5	51.4	29.8	34.1
3-6-OH	76.9	74.7	77.6	74.8	148.8	130.1	99.3	93.6	244.0	46.6	24.3	28.6
3-4′-OH	77.4	75.4	78.0	75.3					244.4	47.2	24.8	29.1
3-3‴-OH	83.8	82.0	84.7	82.5					250.9	53.9	31.4	36.3
3-5‴-OH	83.6	81.8	84.2	82.1					250.7	53.7	31.0	35.9
4-6-OH	79.8	77.9	80.3	78.1	156.9	137.7	105.8	100.7	238.8	42.2	20.5	24.9
4-3″-OH	84.5	82.9	85.3	83.1					243.5	47.2	25.5	29.9
4-5″-OH	83.2	81.6	84.2	82.0					242.2	45.9	24.4	28.8
4-3‴-OH	86.9	84.5	86.0	83.7					245.8	48.8	26.2	30.5
4-5‴-OH	82.9	81.1	83.6	81.5					241.8	45.4	23.8	28.3

Compounds	PA				ETE			
	Gas	Benzene	Methanol	Water	Gas	Benzene	Methanol	Water
1-6-OH	338.1	103.5	51.0	54.0	55.5	74.1	72.6	69.0
1-4′-OH	333.4	100.1	48.8	51.8	60.5	77.8	75.3	71.5
1-3″-OH	336.5	102.4	49.9	52.8	64.5	83.1	81.7	78.1
1-5″-OH	325.9	93.0	52.1	54.1	72.8	98.1	88.3	84.6
1-3‴-OH	325.9	109.6	52.1	54.1	76.5	76.7	89.9	86.1
1-5‴-OH	342.7	107.8	53.3	56.1	55.8	75.1	76.2	72.7
2-6-OH	337.2	102.0	49.5	52.4	55.3	74.6	73.3	69.6
2-4′-OH	342.0	105.4	51.6	54.5	50.5	71.2	71.1	67.5
2-3″-OH	345.3	107.7	52.6	55.4	48.5	70.2	71.5	67.9
2-5″-OH	345.0	107.3	52.4	55.3	54.4	76.5	77.9	74.4
3-6-OH	339.6	104.2	51.9	54.2	53.2	72.5	71.7	68.0
3-4′-OH	334.4	100.4	49.4	51.8	58.8	76.9	74.7	70.9
3-3‴-OH	344.5	107.1	52.8	55.6	55.2	77.0	77.9	74.3
3-5‴-OH	344.0	106.7	52.5	55.4	55.5	77.1	77.8	74.2
4-6-OH	339.8	104.1	50.2	53.1	55.9	75.8	75.0	71.4
4-3″-OH	338.3	103.1	51.3	54.1	62.1	81.8	81.1	77.5
4-5″-OH	327.5	93.7	52.1	54.1	71.6	89.9	88.1	84.4
4-3‴-OH	327.6	91.5	52.2	54.5	75.2	95.0	89.7	86.0
4-5‴-OH	341.6	106.3	53.1	56.0	57.1	76.8	76.5	73.0

the SPL-ET route. Hence, the detailed analysis of the IP and PA numbers is very important. Taking the computational IP enthalpy into account, this value of each compound orderly ranks as gas > benzene > methanol > water. Our previous DFT calculation on the analogous benzofuran-stilbene hybrid derivatives also indicated that the increase of solvent's polarity will cause the decrease of the IP values [17]. The IP values in each solvent of compound **3** (the deletion of ring D) are comparable with compound **1**, and the lowest values of 94.2 and 93.6 kcal/mol are assigned to compounds **1** and **3** in water, respectively (Table 1). However, converted natural product **1** into synthetic compounds **2** (the deletion of ring E

and double bond) and **4** (the deletion of ring B) did not promote the IP reduction.

The second stage of the SPL-ET route is due to deprotonation of cation radical X-OH$^{\bullet+}$ and is characterized by the PDE enthalpies. It turns out that the computational OH PDE values of four studied compounds **1-4** have dropped dramatically when transferred gas into liquids. Furthermore, the methanolic and aqueous PDE enthalpies are 1.5–2 times lower than those in benzene. An order for the PDE values is visualized as gas >> benzene > water > methanol. It resembles the BDE; the PDE enthalpies of 6-OH and 4′-OH of each compound are found lower than those of the remaining OH groups in each medium. The lowest and highest PDE enthalpies belong to **4**-6-OH (20.5 kcal/mol) in methanol and **1**-3‴-OH (254.8 kcal/mol) in gas, respectively. The findings on the PDE calculation are in agreement with our previous result [17], in which solvents, like methanol and acetone, seem to support the PDE reduction of benzofuran-stilbene hybrids better than strong polar water or weak polar benzene and nonpolar gas.

The first stage in the SPL-ET route is related to the computational PA enthalpies. The effects of environmental change on the PA outcomes are significant. The selection of polar solvents, like methanol and water, seems to be the best way to decrease the PA values. Indeed, the PA calculations assigning to OH groups of compounds **1-4** are always found in the consistent order methanol < water < benzene << gas. In agreement with literature compounds, at the same theoretical DFT/B3LYP/6-311G(d,p) level, the calculated approaches on well-known antioxidative flavonoids suggested that this chemical class has also generated the low PA values in water and much better than in gas or benzene [20, 21].

In other assessments, in methanol and water, 6-OH groups of compounds **1-4** and 4′-OH of compounds **1-3** should be centers of antiradical reactions since they reached the PA values lower than the other OH groups in each compound. As compared natural compound **1** to synthetic compounds **2-4**, **1**-4′-OH with the lowest PA value of 48.8 kcal/mol evidently indicated that the use of natural products type benzofuran-stilbene hybrid compounds to antioxidative treatments gets more efficacious than the application of the synthetic analogs.

Considering the second stage of SPL-ET route, the ETE calculations will be characteristic of electron transmission. For Table 1, the arrangement of the ETE values of each OH bond breakage is always run as gas < water < methanol < benzene. It can be proposed that the polarity of medium is the key factor for the electron transfer. **2**-3″-OH and **1**-5″-OH achieve the lowest and highest ETE values of 48.5 and 98.1 kcal/mol in gas and benzene, respectively. It is similar to the IP trend, as compared to compound **1**, the deletion of ring D responses for the ETE decrease in compound **3**, but the disappearances of ring B or ring E fail to do so. Taken together, semi-synthesis aimed to convert the bulk natural product **1** into compound **3**; on the one hand, promote electron transfer; and on the other hand, reduce molecular size.

Preferable mechanisms

The favorable antioxidative mechanisms of four compounds **1-4** have been determined using the BDE, IP, and PA enthalpies computed according to Eqs. (2), (4), and (7). The lower the energies of these descriptors are, the more likely the associated mechanism is [10–17]. Apparently, the SPL-ET route is preferable thermochemically in polar solvents since the PA values in methanol and water are less than the IP and BDE values. However, it turns out that the HAT mechanism will be more favorable than the two remaining mechanisms if the antioxidative reactions happen in the gaseous phase.

The kinetic study

As above discussed, the antioxidative activity of the studied compounds **1-4** has preferentially happened through the SPL-ET mechanism in aprotic solvents. However, it is necessary to interpret how free radicals attack OH groups. In this scenario, a model of HOO$^{\bullet}$ + compounds **1-4** in methanol at the same B3LYP/6-311G(d,p) level is proposed for kinetic consideration since HOO$^{\bullet}$ was a harmful agent present in both living bodies and outside [12]. As can be seen from Eq. 18, the capture of HOO$^{\bullet}$ radicals by compounds **1-4** is promoted since the $\Delta G^{\#}$ value is lower and the K value is higher [10–17]. HOO$^{\bullet}$ + compounds **1-4** mostly include two intermediates (Int-1 and Int-2) and one transition states (TS) (Table 2 and Fig. 2 and Fig. S6). The $\Delta G^{\#}$ and K values make a high agreement with the above thermal calculations, in which, once again, 6-OH and 4′-OH groups of each compound possess the lower $\Delta G^{\#}$ values of 5.6–8.2 kcal/mol and the higher K values of 1.386×10^{9}–1.983×10^{10} L/mol.s, whereas these values assigning to the remaining OH groups are to be the $\Delta G^{\#}$ = 10.1–15.2 kcal/mol and the $K = 8.519 \times 10^{5}$–1.983×10^{10} L/mol.s. **1**-6-OH has generated the lowest $\Delta G^{\#}$ value of 5.6 kcal/mol and the highest K value of 1.983×10^{10} L/mol.s. The K value of **1**-6-OH is found 10^{1}–10^{5} times higher than that of other cases. Also concerned is that among all cases, **1**-6-OH contains TS with the lowest relative energy of −3.8 kcal/mol (Fig. 2). Therefore, the general conclusion of these key points is that the antioxidative actions of benzofuran-stilbene hybrid compounds are mostly contingent upon OH groups directly substituting benzofuran nucleus rather than OH groups of side chains. Our previous publication suggested that OH groups of ring B of similar compounds were antioxidative centers [17]. It confirms that structural feature is a key factor to effect antioxidative results. In addition, the transformation of compound **1** into compounds **2-4** did not promote the $\Delta G^{\#}$ decrease and the K increase of each corresponding OH group. Thus, natural products type benzofuran-stilbene hybrid

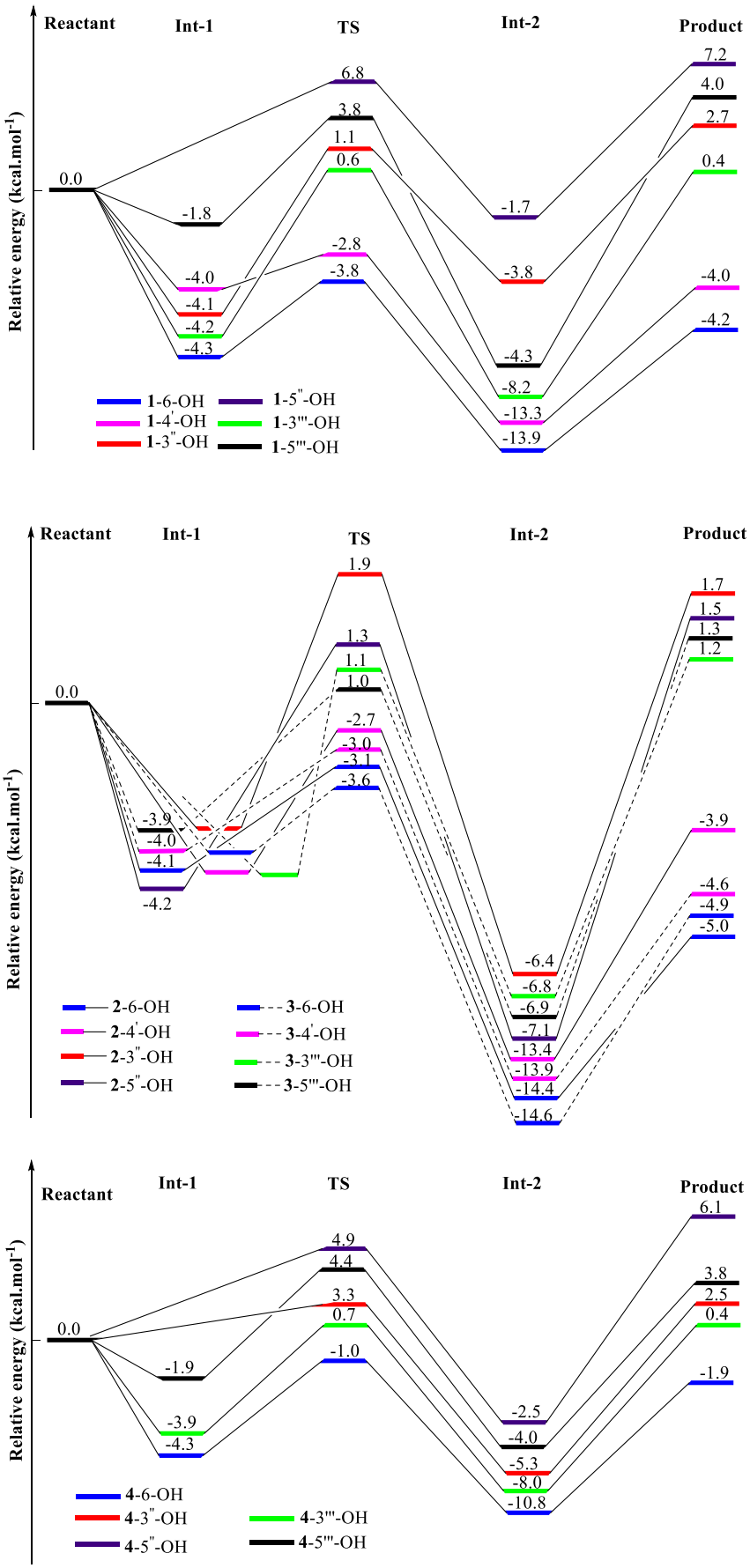

Fig. 2 Energy diagram for the reaction of HOO• radicals attack to compounds **1-4** at the B3LYP/6-311G(d,p) level

Table 2 In the methanol phase and 298.15K, the calculated $\Delta G^{\#}$ and k at the B3LYP/6-311G level for $HOO^{\bullet}$ radical attack

Position	$\Delta G^{\#}$ (kcal/mol)	k (L/mol.s)	Position	$\Delta G^{\#}$ (kcal/mol)	k (L/mol.s)
1-6-OH	5.6	1.983×10^{10}	**3**-6-OH	6.3	9.109×10^{9}
1-4′-OH	6.6	6.991×10^{9}	**3**-4′-OH	6.9	4.969×10^{9}
1-3″-OH	11.3	5.179×10^{7}	**3**-3‴-OH	11.1	6.563×10^{7}
1-5″-OH	15.2	8.519×10^{5}	**3**-5‴-OH	11.3	5.252×10^{7}
1-3‴-OH	10.6	1.122×10^{8}	**4**-6-OH	8.2	1.386×10^{9}
1-5‴-OH	11.8	3.130×10^{7}	**4**-3″-OH	12.6	1.398×10^{7}
2-6-OH	6.3	9.440×10^{9}	**4**-5″-OH	12.8	1.118×10^{7}
2-4′-OH	6.8	5.663×10^{9}	**4**-3‴-OH	10.1	1.877×10^{8}
2-3″-OH	11.0	7.538×10^{7}	**4**-5‴-OH	11.5	4.441×10^{7}
2-5″-OH	11.0	7.352×10^{7}			

compounds seem to exhibit antioxidative activities better than synthetic analogous compounds.

Metal complex chelation

To date, information on the UV-Vis spectroscopic data of compounds **1-4** is quietly limited. Our current DFT approach applying the TD-DFT/B3LYP/6-311G(d,p) level aims to shed light on the computational values wavelength λ_{max}, vertical transition energy E, and oscillator strength f of these compounds in methanol and gas. In both experiences and theories, methanol and gas should be the best selection for the UV-Vis comparison [17, 22, 23]. Table 3 and Fig. 3 reveal that each studied compound is composed of two main λ_{max} peaks due to transition type $\pi \rightarrow \pi^*$, whose λ_{max} values range from 251 to 417 nm in methanol and from 266 to 405 nm in gas. Transition H → L (> 93%) is responsible for the longest λ_{max} in each compound. Taking compound **1** as a typical instance, the methanolic longest λ_{max} of 407 nm (E_{vert} = 3.050 eV, f = 0.711) is mainly caused by H → L (> 98%). Except for compound **3**, a phenomenal blueshift can be observed when comparing compounds **2** and **4** to compound **1** (λ_{max} decreases, E_{vert} increases) [17].

The high accumulative reports have evidenced that metal-chelation is also representative of radical quenching propensity of phenolic compounds [24, 25]. Mostly based on the above thermal and kinetic calculated results, we then propose the complex model [Zn(compound **1**)$_2$(H_2O)$_2$] by covalent bonds of **1**-6-OH group to Zn in methanol (Fig. 4). The FMO and UV-Vis analyses seem likely to be prompt models to view the successful formation of complex [10]. The B3LYP/6-311G(d,p)/LANL2DZ level was used for the optimized procedure and the FMO consideration, whereas for the UV-Vis calculations, TD-DFT method coupled with the functional B3LYP using 6-311G(d,p) basis set for light atoms H, C, and O and LANL2DZ basis set for metal Zn [10, 17]. The difference between compound **1** and its complex can be deduced from their optimized structures (Fig. S1 and Fig. 4).

Table 3 Selectively experimental (methanol) and calculated electronic transitions (methanol and gas) of the studied compounds **1-4**: wavelength λ_{max} (nm), vertical transition energy E (eV), and oscillator strength f, at the TD-DFT/B3LYP/6-311G(d,p) level

No	Methanol				Gas				
	λ_{max} (nm)	E_{vert} (eV)	Oscillator strength f	Transition	λ_{max} (nm)	E_{vert} (eV)	Oscillator strength f	Transition	Transition type
1	407	3.050	0.711	H → L (98%)	392	3.167	0.631	H → L (97%)	π →π*
	320	3.869	0.160	H → L (59%)	294	4.217	0.175	H-3 → L (44%)	
2	336	3.695	0.626	H → L (97%)	329	3.769	0.520	H → L (95%)	
	251	4.934	0.236	H-3 → L (54%)	262	4.729	0.135	H-2 → L (39%)	
3	417	2.972	0.799	H → L (99%)	405	3.064	0.645	H → L (97%)	
	308	4.028	0.592	H → L+1 (73%)	303	4.096	0.313	H → L+1 (42%)	
4	365	3.393	0.564	H → L (96%)	353	3.510	0.420	H → L (93%)	
	262	4.734	0.043	H → L+1 (46%)	266	4.660	0.059	H-2 → L+1 (48%)	
Complex	424	2.926	0.334	H → L (69%)					
	334	3.709	0.542	H-2 → L (45%)					

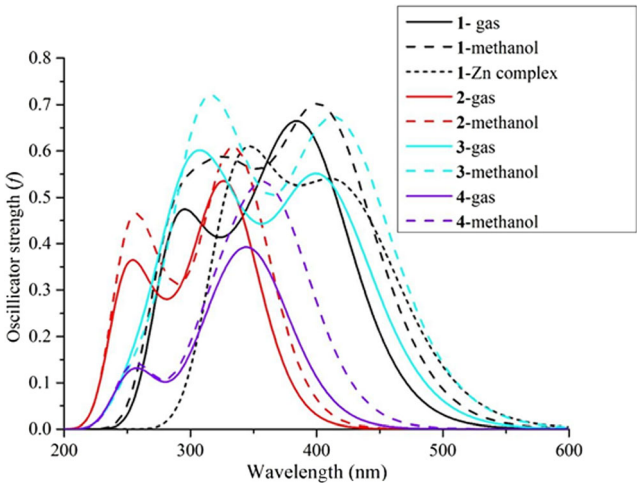

Fig. 3 The UV-Vis absorption of compounds **1-4** at the TD-DFT/B3LYP/6-311G(d,p) level and complex [Zn(compound **1**)$_2$(H_2O)$_2$] at the TD-DFT/B3LYP/6-311G(d,p)/LANL2DZ level

Ring E in complex is capable of binding to ring D via intramolecular hydrogen bond. Zn-O bond lengths reach 1.977–2.094 Å, and OZnO angles run from 84.12 to 95.90°. The electrons are mostly focused on two benzofuran units of HOMO, especially in 6-O atoms, whereas LUMO is presented with the high electrons on one side. Band gap energy of complex [Zn(compound **1**)$_2$(H_2O)$_2$] is lower than single-molecule **1** by 0.142 eV. Regarding the UV-Vis, complex also consists of λ_{max} 424 nm [E_{vert} = 2.926 eV, f = 0.334, and H → L (69%)] and λ_{max} 334 nm [E_{vert} = 3.709 eV, f = 0.542, and H-2 → L (45%)]. The complex formation is associated with phenomenal redshift.

Conclusion

In this paper, we first apply the DFT method to investigate the radical scavenging capacity of compounds **1-4** through thermodynamic and kinetic models. Environment has a significant impact on the outcomes, in which the most preferred mechanism in gas is one-step hydrogen atom transfer (HAT), whereas the SPL-ET mechanism is highly suitable in aprotic solvents methanol and water. The analyses of physicochemical descriptors, such as FMO and spin density, indicated that the antioxidative actions of the studied compounds **1-4** are mainly based on OH bond breakage. At the theoretical B3LYP/6-311G(d,p) level, the natural product type benzofuran-stilbene hybrid compound **1** exhibits the radical scavenging activity better than synthetic compounds **2-4**. 6-OH and 4′-OH of each compound might be the most active sites. Regarding thermal analysis, **1**-6-OH possesses the BDE values of 75.5–77.8 kcal/mol in gas, benzene, methanol, and water and the PA values of above 50.0 kcal/mol in methanol and water. In the kinetic reaction with

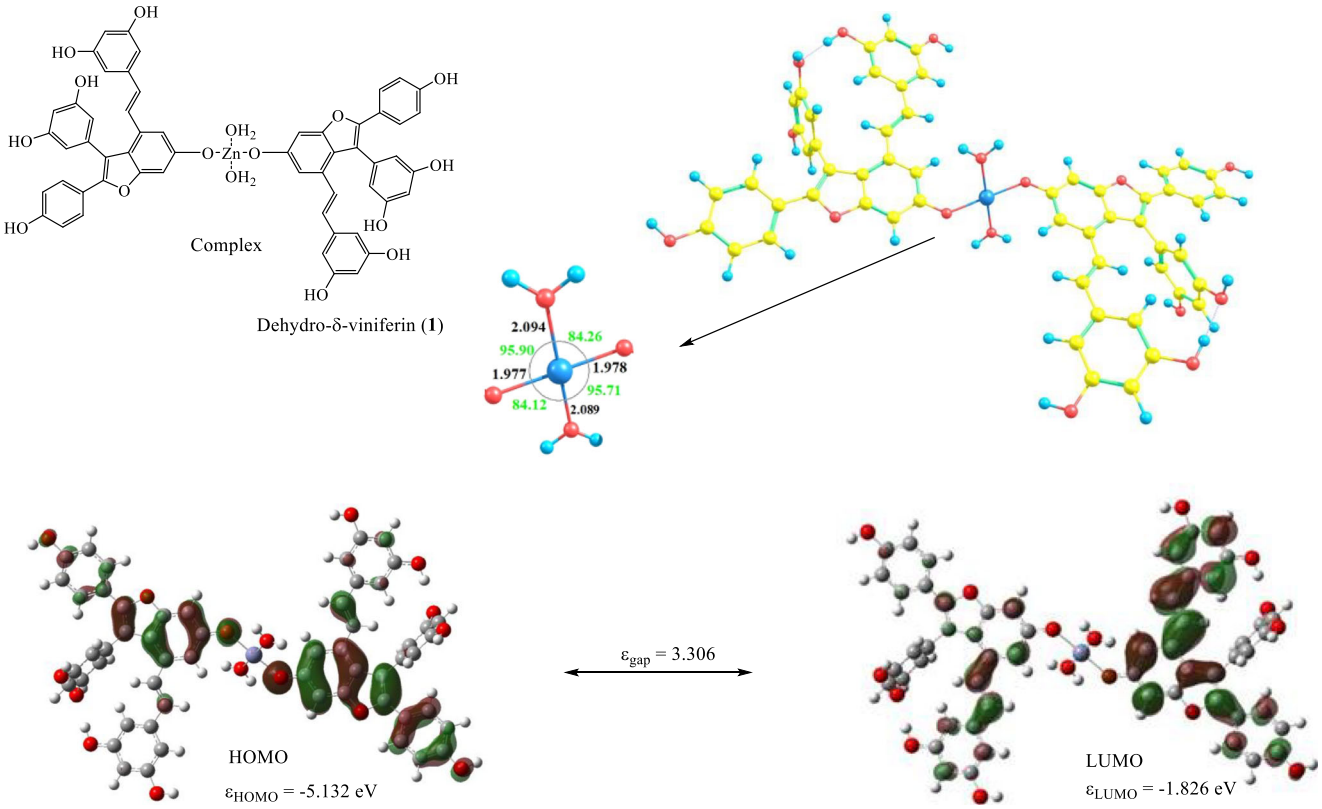

Fig. 4 The optimized complex [Zn(compound **1**)$_2$(H_2O)$_2$] and its FMO illustration in methanol at the B3LYP/6-311G(d,p)/LANL2DZ level

HOO•, **1**-6-OH further induces the lowest $\Delta G^{\#}$ value of 5.6 kcal/mol and the highest *K* value of 1.983×10^{10} L/mol.s. [Zn(compound **1**)$_2$(H_2O)$_2$] causes redshift in methanol at the theoretical B3LYP/6-311G(d,p)/LANL2DZ level in the UV-Vis spectroscopy. This study can be seen as a good starting point for experimental explorations.

Supplementary Information The online version contains supplementary material available at https://doi.org/10.1007/s11224-021-01802-1.

Author contribution Dr. Ninh The Son designed and wrote the manuscript, and Dr. Phan Thi Thuy, Nguyen Van Trang, and Dau Xuan Duc calculated.

Funding This work was financed by the Vietnam Academy of Science and Technology 2021 and Vinh University 2021.

Data availability The data used to support the findings of this study are available from the corresponding author upon request.

Code availability Gaussian 09 package program.

Declarations

Ethics approval Our manuscript has not been submitted to more than one journal for simultaneous consideration. Our manuscript has not been published previously (partly or in full). A single study is not split up into several parts to increase the quantity of submissions and submitted to various journals or to one journal over time (e.g., "salami publishing"). No data have been fabricated or manipulated (including images) to support your conclusions. No data, text, or theories by others are presented as if they were the author's own ("plagiarism"). Proper acknowledgments to other works must be given (this includes material that is closely copied (near verbatim), summarized, and/or paraphrased), quotation marks are used for verbatim copying of material, and permissions are secured for material that is copyrighted.

Consent to participate Our current study did not involve human subject and has not used living animals, etc.

Conflict of interest The authors declare no competing interests.

References

1. Son NT, Thanh DTM, Trang NV (2019) Flavone norartocarpetin and isoflavone 2'-hydroxygenistein: a spectroscopic study for structure, electronic property and antioxidant potential using DFT (density functional theory). J Mol Struct 1193:76–88
2. Dung NT, Thanh DM, Huong NT, Thuy PT, Hoan NT, Thanh DTM, Trang NV, Son NT (2020) Quinolone and isoquinolone alkaloids: the structural-electronic effects and the antioxidant mechanisms. Struct Chem 31:2435–2450
3. Huang KS, Lin M (1999) Oligostilbenes from the roots of *Vitis amurensis*. J Asian Nat Prod Res 2:21–28
4. Huang KS, Lin M, Yu LN, Kong M (2000) Four novel oligostilbenes from the roots of *Vitis amurensis*. Tetrahedron 56: 1321–1329
5. Ha DT, Kim H, Thuong PT, Ngoc TM, Lee I, Hung ND, Bae KH (2009) Antioxidant and lipoxygenase inhibitory activity of oligostilbenes from the leaf and stem of *Vitis amurensis*. J Ethnopharmacol 125:304–309
6. Catinella G, Mattio LM, Musso L, Arioli S, Mora D, Beretta GL, Zaffaroni N, Pinto A, Dallavalle S (2020) Structural requirements of benzofuran derivatives dehydro-δ- and dehydro-ε-viniferin for antimicrobial activity against the foodborne pathogen *Listeria monocytogenes*. Int J Mol Sci 21:2168
7. Fan Y, Zhang Z, Yao C, Bai J, Yang H, Ma P, Fan Y, Li S, Yuan J, Lin M, Hou Q (2019) Amurensin H, A derivative from resveratrol, ameliorates lipopolysaccharide/cigarette smoke induced airway inflammation by blocking the Syk/NF-KB pathway. Front Pharmacol 10:1157
8. Frisch MJ, Trucks GW, Schlegel HB, Scuseria GE, Robb MA, Cheeseman JR, Scalmani G, Barone V, Mennucci B, Petersson GA, Nakatsuji H, Caricato M, Li X, Hratchian HP, Izmaylov AF, Bloino J, Zheng G, Sonnenberg JL, Hada M, Ehara M, Toyota K, Fukuda R, Hasegawa J, Ishida M, Nakajima T, Honda Y, Kitao O, Nakai H, Vreven T, Montgomery JA, Peralta JE, Ogliaro F, Bearpark M, Heyd JJ, Brothers E, Kudin KN, Staroverov VN, Keith T, Kobayashi R, Normand J, Raghavachari K, Rendell A, Burant JC, Iyengar SS, Tomasi J, Cossi M, Rega N, Millam JM, Klene M, Knox JE, Cross JB, Bakken V, Adamo C, Jaramillo J, Gomperts R, Stratmann RE, Yazyev O, Austin AJ, Cammi R, Pomelli C, Ochterski JW, Martin RL, Morokuma K, Zakrzewski VG, Voth GA, Salvador P, Dannenberg JJ, Dapprich S, Daniels AD, Farkas O, Foresman JB, Ortiz JV, Cioslowski J, Fox DJ (2010) Gaussian 09 (revision C.01) Inc., Wallingford CT
9. Phan TT, Son NT (2021) The conversion of L-lysine into L-β-lysine: the role of 5′-deoxyadenosyl radical and water-a DFT study. J Mol Model 27:6
10. Thuy PT, Son NT (2021) Thermodynamic studies on antioxidative action of cynandione A: a DFT approach. Struct Chem. https://doi.org/10.1007/s11224-021-01756-4
11. Anh LTT, Son NT, Tuyen NV, Thuy PT, Quan PM, Ha NTT, Tra NT (2021) Antioxidative and α-glucosidase inhibitory constituents of *Polyscias guilfoylei*: experimental and computational assessments. Mol Divers. https://doi.org/10.1007/s11030-021-10206-6
12. Son NT, Thuy PT, Trang NV (2021) Antioxidative capacities of stilbenoid suaveolensone A and flavonoid suaveolensone B: a detailed analysis of structural-electronic properties and mechanisms. J Mol Struct 11224:12902
13. Phan TT, Son NT (2020) Antioxidant of *trans*-resveratrol: a comparison between OH and CH groups based on thermodynamic views. J Chemother 2020:ID 8869023
14. Thuy PT, Trang NV, Son NT (2020) Antioxidant of 2-phenylbenzofuran derivatives: Structural-electronic effects and mechanisms. RCS Adv 10:6315–6332
15. Elshamy AI, Hama M, Trang NV, Son NT, Okamoto Y, Noji M, Ban S, Umeyama A (2020) A new cerebroside from the endophytic fungus *Ophiocordyceps longiissima*: structural-electronic and antioxidant relations. Experimental and DFT calculated studies. J Mol Struct 1200:127061
16. Son NT, Thanh DM, Trang NV (2019) Isoflavones and isoflavone glycosides: structural-electronic properties and antioxidant relations. A case of DFT study. J Chemother 2019:ID 4360175.
17. Trang NV, Thuy PT, Thanh DTM, Son NT (2021) Benzofuran-stilbene hybrid compounds: an antioxidant assessment – a DFT study. RCS Adv 11:12971–12980
18. Cai W, Chen Y, Xie L, Zhang H, Hou C (2014) Characterization and density functional theory study of the antioxidant activity of quercetin and its sugar-containing analogues. Eur Food Res Technol 238:121–128

19. Sadasivam K, Kumaresan R (2011) Theoretical investigation on the antioxidant behavior of chrysoeriol and hispidulin flavonoid compounds – A DFT study. Computat Theor Chem 963:227–235
20. Senthil Kumar K, Kumaresan R (2012) A DFT study on the structural, electronic properties and radical scavenging mechanisms of calycosin, glycitein, pratensein and prunetin. Computat Theor Chem 985:14–22
21. Boulebd H (2020) Theoretical insights into the antioxidant activity of moracin T. Free Radic Res 54:221–230
22. Son NT, Kamiji M, Huong TT, Kubo M, Cuong NM, Fukuyama Y (2019) Chemical constituents of the Vietnamese plants *Dalbergia tonkinensis* Prain and *Cratoxylum formosum* (Jack) Dyer in Hook and their antioxidative activities. Med Chem Res 28:1441–1447
23. Tra NT, Cham BT, Ha NTT, Anh LTT, Tuyen NV, Son NT (2020) Antioxidant constituents from stem and leaf of *Helicteres hirsuta* Loureiro. Nat Prod J. https://doi.org/10.2174/2210315510999200728131328
24. Abeen E, Janjua NK, Ahmed S, Murtaza I, Ali T, Hameed S (2017) Radical scavenging propensity of Cu^{2+}, Fe^{3+} complexes of flavonoids and in-vivo radical scavenging by Fe^{3+}-primuletin, Spectrochim. Acta A Mol Biomol Spectrosc 171:432–438
25. Miller NJ, Castelluccio C, Tijburg L, Rice-Evans C (1996) The antioxidant properties of theaflavins and their gallate esters-radical scavengers or metal chelators. FEBS Lett 392:40–44

Terms and Conditions

Springer Nature journal content, brought to you courtesy of Springer Nature Customer Service Center GmbH (“Springer Nature”).
Springer Nature supports a reasonable amount of sharing of research papers by authors, subscribers and authorised users (“Users”), for small-scale personal, non-commercial use provided that all copyright, trade and service marks and other proprietary notices are maintained. By accessing, sharing, receiving or otherwise using the Springer Nature journal content you agree to these terms of use (“Terms”). For these purposes, Springer Nature considers academic use (by researchers and students) to be non-commercial.
These Terms are supplementary and will apply in addition to any applicable website terms and conditions, a relevant site licence or a personal subscription. These Terms will prevail over any conflict or ambiguity with regards to the relevant terms, a site licence or a personal subscription (to the extent of the conflict or ambiguity only). For Creative Commons-licensed articles, the terms of the Creative Commons license used will apply.
We collect and use personal data to provide access to the Springer Nature journal content. We may also use these personal data internally within ResearchGate and Springer Nature and as agreed share it, in an anonymised way, for purposes of tracking, analysis and reporting. We will not otherwise disclose your personal data outside the ResearchGate or the Springer Nature group of companies unless we have your permission as detailed in the Privacy Policy.
While Users may use the Springer Nature journal content for small scale, personal non-commercial use, it is important to note that Users may not:

1. use such content for the purpose of providing other users with access on a regular or large scale basis or as a means to circumvent access control;
2. use such content where to do so would be considered a criminal or statutory offence in any jurisdiction, or gives rise to civil liability, or is otherwise unlawful;
3. falsely or misleadingly imply or suggest endorsement, approval , sponsorship, or association unless explicitly agreed to by Springer Nature in writing;
4. use bots or other automated methods to access the content or redirect messages
5. override any security feature or exclusionary protocol; or
6. share the content in order to create substitute for Springer Nature products or services or a systematic database of Springer Nature journal content.

In line with the restriction against commercial use, Springer Nature does not permit the creation of a product or service that creates revenue, royalties, rent or income from our content or its inclusion as part of a paid for service or for other commercial gain. Springer Nature journal content cannot be used for inter-library loans and librarians may not upload Springer Nature journal content on a large scale into their, or any other, institutional repository.
These terms of use are reviewed regularly and may be amended at any time. Springer Nature is not obligated to publish any information or content on this website and may remove it or features or functionality at our sole discretion, at any time with or without notice. Springer Nature may revoke this licence to you at any time and remove access to any copies of the Springer Nature journal content which have been saved.
To the fullest extent permitted by law, Springer Nature makes no warranties, representations or guarantees to Users, either express or implied with respect to the Springer nature journal content and all parties disclaim and waive any implied warranties or warranties imposed by law, including merchantability or fitness for any particular purpose.
Please note that these rights do not automatically extend to content, data or other material published by Springer Nature that may be licensed from third parties.
If you would like to use or distribute our Springer Nature journal content to a wider audience or on a regular basis or in any other manner not expressly permitted by these Terms, please contact Springer Nature at

onlineservice@springernature.com